

RESEARCH

Open Access



Insights of different analytical approaches for estimation of budesonide as COVID-19 replication inhibitor in its novel combinations: green assessment with AGREE and GAPI approaches

Mohammed E. A. Hammouda^{1,2*}, Amal A. El-Masry¹, Saadia M. El-Ashry¹ and Dalia R. El-Wasseef^{1,3}

Abstract

Simple, direct, rapid, and sensitive HPLC and spectrophotometric methods were established for simultaneous estimation of a novel combination of budesonide and azelastine (BUD/AZL) in their laboratory-prepared mixture and dosage form according to the medicinally recommended ratio 1:4.28. Budesonide is an important inhalation corticosteroid that plays a vital role in the inhibition of COVID-19 replication and cytokine production. The first chromatographic method was created for the simultaneous estimation of BUD epimers in the presence of AZL with excellent efficiency in a relatively short chromatographic run (< 9 min). The separation of BUD epimers with AZL was carried out on a C₁₈ column using acetonitrile: phosphate buffer of pH 3.5 adjusted by 0.2 M orthophosphoric acid (40:60, v/v) as a mobile phase, UV detection at 230 nm and a flow rate of regulated at 2 mL/min. Besides, three spectrophotometric methods were applied for the simultaneous determination of the provided mixture adopting zero order, first order derivative, and ratio first derivative approaches. The Zero-order spectrophotometry was used for the determination of AZL in presence of BUD, where BUD shows no absorbance at 290 nm. The first derivative amplitude at 265 nm (¹D₂₆₅) (zero-crossing of AZL) and the ratio of first derivative amplitudes at 270 nm (¹DD₂₇₀) using 10.0 µg mL⁻¹ AZL as divisor was chosen for the simultaneous determination of BUD in the presence of AZL in the binary mixture. The proposed methods were found to be rectilinear in the concentration range of (0.4–40.0 µg mL⁻¹) and (0.05–40.0 µg mL⁻¹) for BUD and AZL, respectively in the HPLC method. Whereas the concentration range for AZL in the zero-order method was (1.0–35.0 µg mL⁻¹) and for BUD in the first derivative and ratio derivative method was (6.0–20.0 µg mL⁻¹). Validation of the suggested approaches according to the ICH criteria was performed. Furthermore, to ensure the proposed approaches' greenness, The AGREE and GAPI metrics were utilized, and the afforded results revealed an excellent greenness of the proposed approaches.

Keywords Azelastine, Budesonide, HPLC, Zero order, First derivative, Ratio first derivative, COVID-19, Inhalation corticosteroids, Allergic rhinitis, AGREE, GAPI

*Correspondence:

Mohammed E. A. Hammouda

drmedo4u@mans.edu.eg; mabdelghafar@horus.edu.eg;

drmo4u@yahoo.com

Full list of author information is available at the end of the article



© The Author(s) 2023. **Open Access** This article is licensed under a Creative Commons Attribution 4.0 International License, which permits use, sharing, adaptation, distribution and reproduction in any medium or format, as long as you give appropriate credit to the original author(s) and the source, provide a link to the Creative Commons licence, and indicate if changes were made. The images or other third party material in this article are included in the article's Creative Commons licence, unless indicated otherwise in a credit line to the material. If material is not included in the article's Creative Commons licence and your intended use is not permitted by statutory regulation or exceeds the permitted use, you will need to obtain permission directly from the copyright holder. To view a copy of this licence, visit <http://creativecommons.org/licenses/by/4.0/>. The Creative Commons Public Domain Dedication waiver (<http://creativecommons.org/publicdomain/zero/1.0/>) applies to the data made available in this article, unless otherwise stated in a credit line to the data.

Introduction

Azelastine (AZL), chemically named as: (4-(4-chlorobenzyl)-2-[(4*RS*)-1-methylhexahydro-1*H*-azepin-4-yl]phthalazin-1(2*H*)-one hydrochloride [1]; Fig. 1b. It is a second generation relatively selective histamine H_1 antagonist, which prevents mast cells implicated in the allergic reaction from releasing histamine and other mediators. AZL has been demonstrated for the inhibition of leukotrienes and platelet-activating factors. Furthermore, it inhibits the accumulation and degranulation of eosinophils at the site of allergic inflammation. It is recommended for the treatment of the symptoms of seasonal allergic rhinitis and conjunctivitis in adults and pediatric patients [1].

Budesonide (BUD), chemically named as (*R,S*)-16 α ,17 α -butylenedioxy-11 β ,21-dihydroxypregna-1,4-diene 3,20-dione [2]; Fig. 1a. is an anti-inflammatory, its affinity for the glucocorticoid receptor is approximately 200-fold greater than that of hydrocortisone and 15-fold greater than that of prednisolone. BUD is available in a combination of two epimers (22*R* and 22*S*) that resulted from adding an alkyl chain at a chiral C_{22} atom, where the ratio range of *R:S* epimers was within 60/40, 51/49 [1]. High glucocorticoid activity is observed in both epimers, with the 22*R* epimer having a twofold higher affinity than the 22*S* epimer [3].

The in vitro data suggests that treatment with the inhaled corticosteroid budesonide in conjunction with bronchodilators inhibits Human coronavirus 229E (HCoV-229E) multiplication and cytokine generation in bronchial epithelial cells, according to recent studies on the pandemic coronavirus [4]. Angiotensin-converting enzyme 2 (ACE2) gene expression is reduced in the sputum of Chronic obstructive pulmonary disease (COPD) and asthma patients who take inhaled corticosteroids (ICS) compared to those who do not [5, 6], suggesting that ICS may also inhibit SARS-CoV-2 penetration. Additionally, research in mice has demonstrated that ICS

decreases ACE2 expression by preventing the production of type 1 Interferon (1 IFN) [5]. The resulting decrease in ACE2 expression may protect SARS-CoV-2 cellular entrance, even while inhibition of type 1 IFN production may impair host defense. These data suggest that the use of ICS especially budesonide in asthmatic and COPD patients may protect against Coronavirus disease 2019 (COVID-19) and be considered an interesting drug candidate for further development [7].

Upon reviewing the literature, it was discovered that several analytical techniques have been published for the determination of BUD in both pure form and pharmaceutical formulations, such as; spectrophotometry [8–12], high-performance liquid chromatography (HPLC) [13–20], liquid chromatography with tandem mass spectrometry (LC/MS/MS) [21], ultra-high performance liquid chromatography with tandem mass spectrometry (UPLC/MS/MS) [22, 23] and gas chromatography (GC) [24]. Moreover different analytical methods were established for the determination of AZL either in pure form or pharmaceutical preparations, such as; spectrophotometry [25–31], spectrofluorimetry [32], electrochemical methods [33–35], TLC [36, 37], HPLC [28, 38–41], high-performance thin layer chromatography (HPTLC) [42], LC/MS/MS [43, 44] and electrokinetic capillary chromatography (EKCC) [44].

A novel combination of (BUD and AZL) significantly relieves allergic nasal symptoms (itchy nose and sneezing) as measured by the total nasal symptom score (TNSS) [45], where the results of scientific research showed that the use of BUD and AZL together led to significant improvements in nasal congestion that occurred more quickly than with either drug used alone in patients with seasonal allergic rhinitis [46].

The effectiveness and novelty of this combination encouraged the establishment of different analytical approaches utilized for the estimation of both drugs in



Fig. 1 Chemical structures of **a** budesonide and **b** azelastine

their synthetic mixture and dosage forms. The innovation of the provided approaches is that there are neither spectrophotometric nor HPLC methods yet have been developed in the literature for their simultaneous estimation. Thus, it was imperative to develop new facile, sensitive, and effective methods for their determination. Different analytical parameters were studied and optimized, furthermore, the greenness of the proposed approaches was ensured by adopting the AGREE and GAPI metrics.

Experimental

Instruments

HPLC separation was performed with Knauer series P 6.1 L Chromatograph equipped with a 20 μ L Rheodyne injector valve and a UV/VIS detector operated at 230 nm. Total Chrom Workstation (Massachusetts, USA) was utilized for the collection and processing of data. The mobile phase filtration was performed by 0.45 μ m membrane filters (Millipore, Ireland). The pH was measured by A Consort P-901 pH meter.

A Lamb America Unico-USA series visible double-beam spectrophotometer (model S1200 equipped with 2 matched 1-cm path-length quartz cells) was adopted for the spectrophotometric analyses.

Reagents and materials

BUD certified as 99.80% purity was kindly provided by Jayco Chemical Industries (Maharashtra, India), and its pharmaceutical preparation Rhinocort Aqua (Contains 32 μ g/dose BUD, Batch no #170183) was obtained from the local pharmacy. Azelastine hydrochloride (AZL) certified as 99.80% purity was provided as a gift by European Egyptian Pharmaceuticals Industry, Alexandria, Egypt, and its pharmaceutical preparation Zalastin Metered Dose Inhaler (labeled to contain 1 mg mL⁻¹ AZL, Batch no #4579004) was obtained from the local pharmacy. (22S)-budesonide (budesonide epimer A) and (22R)-budesonide (budesonide epimer B) were purchased from SimSon Pharma Limited (Mumbai, India). Acetonitrile (of HPLC high grade) was bought from Sigma-Aldrich (Germany). Sodium dihydrogen phosphate product of El-Nasr Pharmaceutical Chemicals (ADWIC), Cairo, Egypt. Orthophosphoric acid was purchased from Prolabo (Paris, France).

Chromatographic condition

The separation was carried out by a Knauer C₁₈ column (150 mm \times 4.6 mm, 5 μ m particle size). The mobile phase consists of acetonitrile: sodium dihydrogen phosphate (0.04 M) of pH 3.5 adjusted by 0.2 M orthophosphoric acid, in the ratio of (40:60, v/v). The filtration was performed with a 0.45 μ m millipore membrane filter and

then degassed by sonication for 10 min before injection. The separation was applied at room temperature using a flow rate of 2 mL/min at wavelength 230 nm.

Procedures

Preparation of standard solutions

Standard stock solutions of (100 μ g mL⁻¹) were created for both BUD and AZL for the utilization in the spectrophotometric methods by dissolving 10 mg of pure drugs into two different 100 mL measuring flasks, and the volume was brought to the mark with acetonitrile. Additional dilutions were carried out for the HPLC procedure to produce the working solutions of (50 μ g mL⁻¹ for each drug). Furthermore, Standard stock solutions of BUD epimer A and epimer B were prepared by dissolving 10 mg individually into two separate 100 mL volumetric flasks, the volume was completed to the mark with the same solvent. When maintained in the refrigerator at 4 °C, the standard solutions were confirmed to be stable for at least a week.

General procedures and construction of calibration graphs

HPLC method Increasing volumes of standard solutions of BUD and AZL were successfully transferred into a series of 10 mL volumetric flasks, yielding solutions with concentrations ranging from (0.4–40.0 μ g mL⁻¹) for BUD and (0.05–40.0 μ g mL⁻¹) for AZL. Moreover, standard solutions of both BUD epimers (Epimer A and B) and AZL were transferred into another series of 10 mL volumetric flasks yielding final solutions with the same concentrations range. Prior to injection, the flasks were filled to the mark with the mobile phase, and 20 μ L were injected in triplicate at room temperature (25 °C). The calibration curves were constructed by plotting the peak areas against the final concentration of the studied drugs, and the regression equations were created.

Spectrophotometric methods In order to obtain solutions with concentrations range of 6.0–20.0 and 1.0–35.0 μ g mL⁻¹ for BUD and AZL, respectively, an increasing volume of the standard solution were transferred to a series of 10 mL measuring flasks, which were then diluted to 10.0 mL with acetonitrile. The zero-order absorption spectra for both drugs were recorded against acetonitrile a blank.

For determination of AZL by zero-order direct spectrophotometric method. The absorbance values of AZL were recorded at 290 nm where; there are no overlapped spectra (no absorbance gathered from BUD).

The first-order derivative values were recorded at 265 nm in order to determine BUD via first-derivative spectrophotometry. The calibration graph was created

by plotting the derivative amplitudes against the drug concentrations, and the associated regression equation was then created.

Moreover, the first derivative of the ratio spectra was recorded (the spectra of BUD divided by the spectrum of $10 \mu\text{g mL}^{-1}$ AZL solution) was recorded. The signal at 270 nm for BUD was measured. The calculated values were then plotted against the final concentrations to generate the calibration graph, from which the relevant regression equation was constructed.

Determination of the studied drugs in their synthetic laboratory-prepared mixture

To create various laboratory-prepared mixtures of BUD and AZL, accurately measured aliquots of the standard solutions of both drugs were transferred into a set of 10 mL volumetric flasks. Different concentrations of both drugs were utilized to get a constant ratio of (1:4.28) for (BUD: AZL), similar to those employed in pharmaceutical formulation. The volume was completed with the mobile phase for the HPLC method and with acetonitrile for spectrophotometric methods, mixed well, and analyzed as indicated under "Construction of calibration graphs" for each method. Finally, the regression equations and their parameters were then calculated and derived statistically.

Application of the proposed methods to the analysis of the studied drugs in their laboratory-prepared dosage form

Into a 25 mL volumetric flask, 10 sprays of rhino aqua (each spray contained $32 \mu\text{g}$ BUD) and 1.37 mL of Zalas-tin nasal spray (each mL contained $1000 \mu\text{g}$ AZL) were transferred, mixed with 15 mL acetonitrile, and sonicated for 10 min. The solution was topped up with acetonitrile, well mixed, filtered, and then proceeded as stated under "Construction of calibration graphs" for each approach.

Results and discussion

A validated chromatographic method was developed for the simultaneous estimation of BUD and AZL. The proposed method provided a highly sensitive and rapid determination of both drugs in their laboratory synthetic mixture and pharmaceutical preparation, as it provided a successful separation with satisfactory resolution ($R_s = 13.16, 1.17$) between BUD, AZL, and between two epimers of BUD, respectively; within a short elution time (less than 9 min, $R_{t_{\text{BUD epimers(B, A)}}} = 8.03, 8.73$ min, $R_{t_{\text{AZL}}} = 2.32$ min) under the optimum selected chromatographic condition as represented in Fig. 2.

The UV absorption spectrum of BUD exhibited maxima at 244 nm and AZL possesses UV absorption maxima at 228 nm, 257 nm, and 290 nm as shown in Fig. 3. Thus, conventional UV spectrophotometry could be used for the determination of AZL at the wavelength of 290 nm in presence of BUD, as there is no absorbance

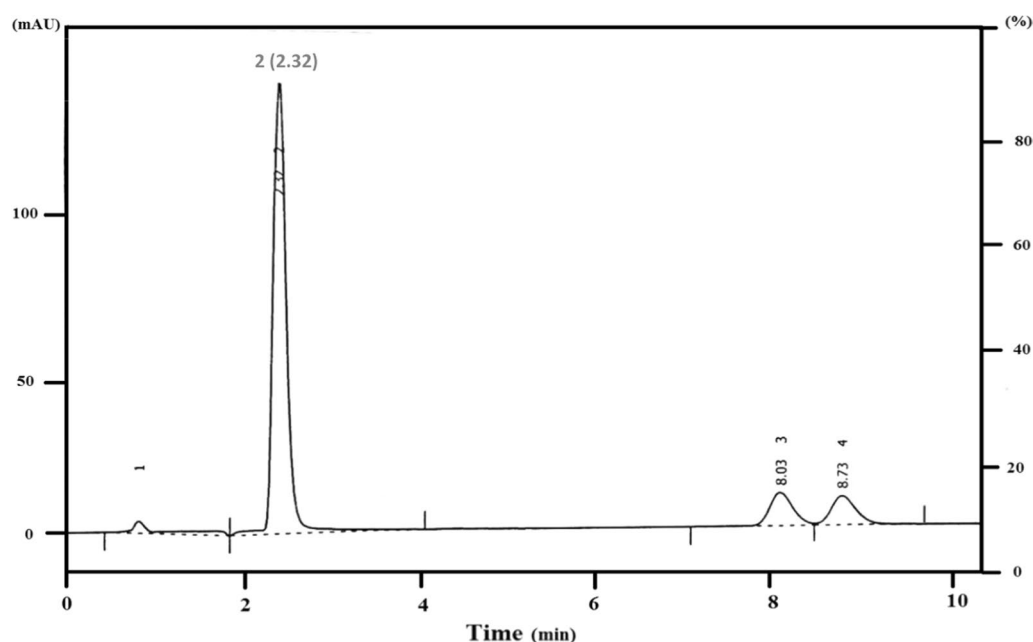


Fig. 2 Typical chromatogram for the separation of BUD ($30 \mu\text{g mL}^{-1}$) [BUD Epimer B; 8.03 min, BUD epimer A; 8.73 min) and AZL ($30 \mu\text{g mL}^{-1}$, 2.32 min)]. Where; (1) solvent front, (2) AZL, (3) BUD epimer B and (4) BUD epimer A

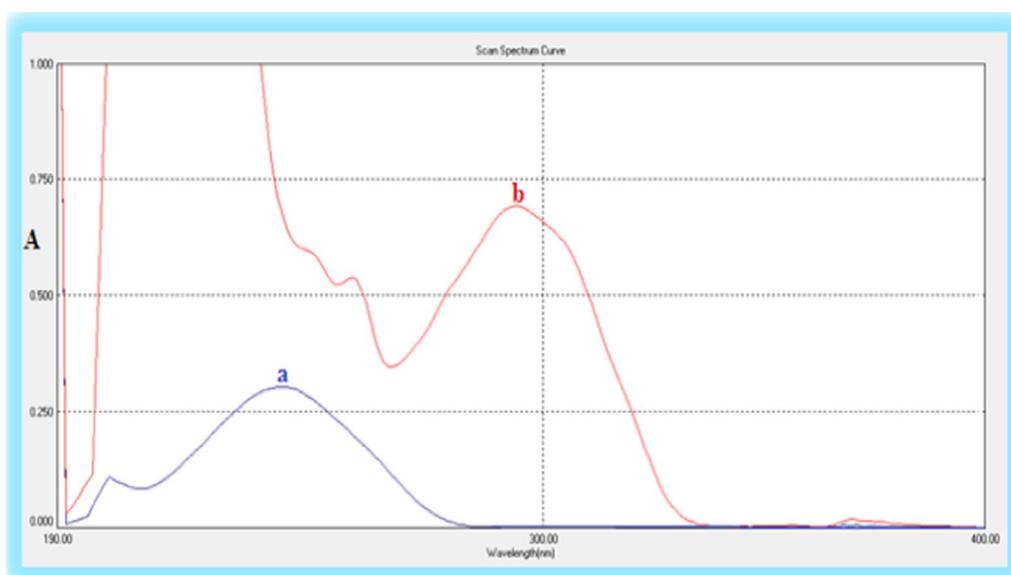


Fig. 3 Absorption spectra of **a** BUD ($6 \mu\text{g mL}^{-1}$) and **b** AZL ($25.0 \mu\text{g mL}^{-1}$) in acetonitrile

observed from BUD at this wavelength. On the other hand, BUD couldn't be measured at the wavelength of 244 nm due to overlapped spectra, so the first derivative and ratio first derivative methods were suggested for simultaneous estimation of both drugs without any interference from each other.

The first derivative spectra of both BUD and AZL exhibit aspects that may allow the successful determination of BUD in the presence of AZL as shown in Fig. 4. the first derivative intensity at 265 nm (zero-crossing of AZL) was chosen for the simultaneous estimation of BUD in the presence of AZL in the binary mixture.

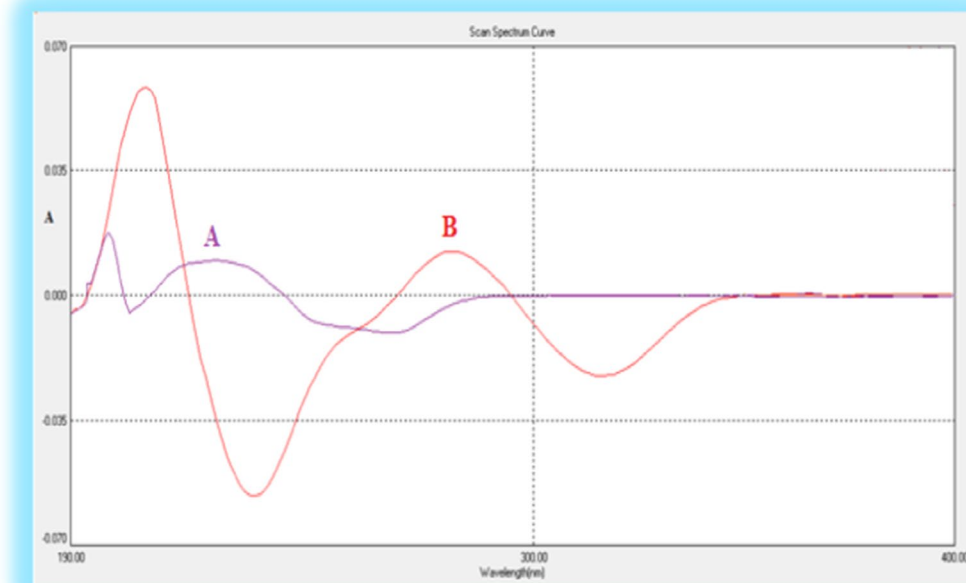


Fig. 4 First-order derivative spectra of **a** $6 \mu\text{g mL}^{-1}$ BUD and **b** $25 \mu\text{g mL}^{-1}$ AZL in acetonitrile, where BUD measured at 265 nm (zero crossing for AZL)

In the ratio first derivative spectrophotometry, the first derivative of the ratio spectra of various BUD concentrations (spectra divided by the spectrum of a solution containing $10.0 \mu\text{g mL}^{-1}$ of AZL) was shown in Fig. 5. Where, the intensity at 233 or 270 nm ($^1\text{DD}_{233, 270}$) in the ratio derivative spectra represent BUD that exists in the solution, so it can be used for its estimation.

As it directly affects the spectral shape, bandwidth, and signal value, the optimal $\Delta\lambda$ value is a critical determinant while conducting the first derivative of the ratio spectra, as a result, several values were investigated. It was found that $\Delta\lambda=7 \text{ nm}$ gave the best shape, the maximum absorbance values, and the best-separated peaks so, it was selected to determine BUD in presence of AZL. Various concentrations were investigated, and various calibration curves were produced, with the purpose of identifying the standard solution as a divisor. Spectra of $10.0 \mu\text{g mL}^{-1}$ AZL was used as a divisor for the determination of BUD, the best results in terms of sensitivity, signal-to-noise ratio, and repeatability were achieved.

Optimization of the chromatographic condition

The performance of the utilized chromatographic system of the investigated combination was affected by several parameters, which were evaluated in order to

determine the optimum conditions that achieve an efficient separation with satisfactory results.

UV-detection

The UV absorption spectra of the investigated drugs exhibited maximum absorption at 244 nm for BUD and 228, 290 nm for AZL (Fig. 3). During the laboratory investigations, several wavelengths were evaluated at 210, 220, 230, 240, 250, and 254 nm. The wavelength at 230 nm was chosen as it shows the highest sensitivity for both drugs.

Mobile phase composition

Different alterations in the composition mobile phase were considered so as to change the selectivity of the chromatographic system to provide efficient separation of not only BUD and AZL but also the two epimers of BUD; these modifications include:

Type of organic modifier Several organic modifiers including (methanol and acetonitrile) were investigated to choose the best for the separation. Acetonitrile was chosen, as it allowed separation in shorter elution time with symmetrically good-resolved peaks. On the other side, methanol resulted in band broadening and retardation for both BUD and AZL.

The ratio of organic modifier The influence of different ratios of acetonitrile on the separation efficiency

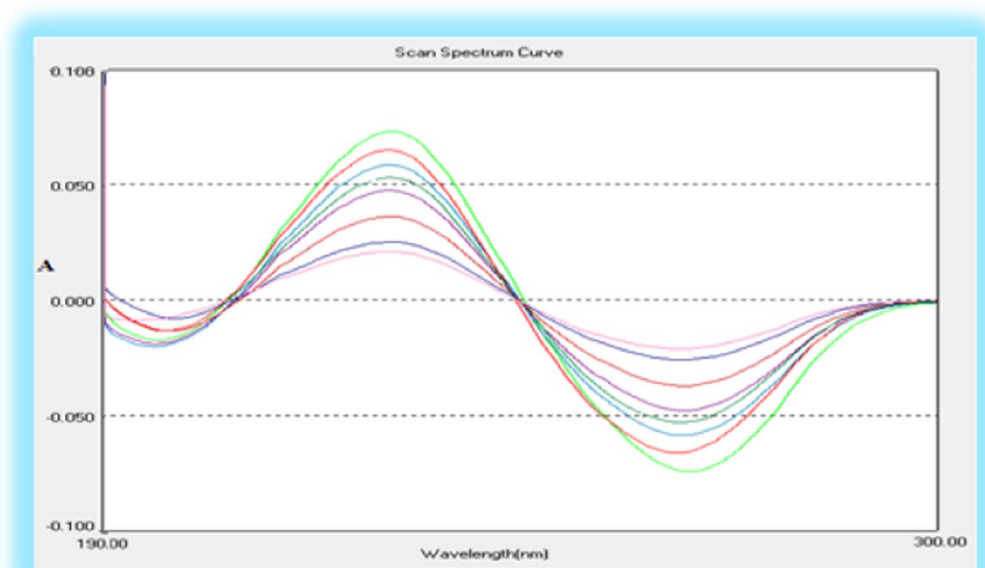


Fig. 5 First derivative of the ratio spectra of BUD (6, 8, 10, 12, 14, 16, 18 and $20 \mu\text{g mL}^{-1}$) when $10.0 \mu\text{g mL}^{-1}$ AZL was used as divisor (at 233, 270 nm)

of eluted drugs was tested in the range of (30–50%). It was found that changing the ratio of organic modifier has a great influence on separation on both drugs, and on the two epimers of BUD, as above 42% of acetonitrile, poor separation of both epimers of BUD was gained, as their resolution was less than 1. Below 40% of acetonitrile, both epimers of BUD were retained to unacceptable retention time with lower separation efficiency as revealed by N for both BUD and AZL. So, 40% of acetonitrile was used as the optimum ratio with 60% (0.04 M) of sodium dihydrogen phosphate as shown in Table 1.

The pH of the mobile phase The effect of pH of the mobile phase was investigated across the range (3.0–6.0) by utilizing (0.2 M) orthophosphoric acid. By reviewing the literature it was found that BUD has a log P of 2.73 and a pKa of 13.74 [47], while AZL has a Log P of 3.5 [48] and a pKa of 8.88 [39]. The proposed study revealed that as the pH of the mobile phase was elevated, the AZL peaks appeared unsymmetrical and broader with increased elution time, while BUD was not significantly affected by pH where it was assumed to be fully unionized over the investigated pH range while AZL is ionized and elute very rapid. So, pH 3.5 was selected as the optimum pH for separation, as well-defined symmetrical peaks were eluted with adequate resolution and appropriate elution times as shown in Fig. 2, Table 1.

The ionic strength of phosphate buffer The effect of the different molar concentrations of phosphate buffer on the separation efficiency of eluted drugs was performed in the range from (0.02–0.05 M) at a fixed ratio of (60% phosphate buffer: 40% acetonitrile, v/v), 0.04 M phosphate buffer was chosen as it provided the best separation with the highest efficiency in adequate elution time and appropriate selectivity as shown in Table 1.

Flow rate

The flow rate was likewise evaluated from 1.5 to 2.2 mL/min. A flow rate of 2 mL/min was selected as the optimum flow rate afforded efficient separation in an appropriate elution time; below this flow rate, an increased run time was achieved with low sensitivity; above it, the two epimers of BUD were badly resolved from each other, also AZL was co-eluted with solvent front.

The optimum chromatographic condition affected the efficiency of separation of BUD and AZL was achieved by a mobile phase constituted of acetonitrile: sodium dihydrogen phosphate of pH 3.5 adjusted by 0.2 M orthophosphoric acid (40:60, v/v) with flow rate 2 mL/min.

Analytical performance

The suggested approaches were validated in accordance with ICH Q2 (R1) guidelines [49] concerning the following validation criteria.

Linearity and range

The peak area and the drug concentration across the range are correlated linearly throughout the range of (0.4–40.0 $\mu\text{g mL}^{-1}$) and (0.05–40.0 $\mu\text{g mL}^{-1}$) for BUD and AZL, respectively in the HPLC method and between (derivative amplitude & absorbance) and drug concentration throughout the range of (6.0–20.0 $\mu\text{g mL}^{-1}$) and (1.0–35.0 $\mu\text{g mL}^{-1}$) of BUD and AZL, respectively in spectrophotometric methods. Calibrations of both pure epimers (A and B) were performed separately, and their regression equations were derived (Eqs. 1 and 2). Furthermore, the overall BUD concentration was calculated by summation of the AUC of both peaks of the two epimers consequently the data was applied to the linear regression analysis, and Eq. (3) was developed (Table 2).

Table 2 displayed analytical performance data for determining BUD and AZL. The following equations were developed by linear regression analysis of the data gathered using the described techniques:

$$\begin{aligned} \text{For HPLC method: PA} &= -0.07 + 13.31 C \\ (r &= 0.9999) \\ \text{For BUD epimer B only,} & \end{aligned} \quad (1)$$

$$\begin{aligned} \text{For HPLC method: PA} &= -0.29 + 13.31 C \\ (r &= 0.9999) \\ \text{For BUD epimer A only,} & \end{aligned} \quad (2)$$

$$\begin{aligned} \text{For HPLC method: PA} &= -0.36 + 13.31 C \quad (r = 0.9999) \\ \text{For BUD (epimer A + B),} & \end{aligned} \quad (3)$$

$$\begin{aligned} \text{For HPLC method: PA} &= 0.89 + 47.48 C \\ (r &= 0.9999) \quad \text{For AZL.} & \end{aligned} \quad (4)$$

For the first derivative:

$$\text{DA} = 18 \times 10^{-4} + 17 \times 10^{-4} C \quad (r = 0.9999)$$

For BUD at 265 nm ($^1\text{D}_{265}$),

For the ratio first derivative:

$$\text{DA} = -19 \times 10^{-4} + 38 \times 10^{-4} C \quad (r = 0.9999)$$

For BUD at 270 nm ($^1\text{DD}_{270}$),

For the zero order:

$$\text{A} = 34 \times 10^{-3} + 26 \times 10^{-3} C \quad (r = 0.9999)$$

For AZL at 290 nm.

Table 1 Optimization of chromatographic performance for simultaneous separation of BUD epimers and AZL by HPLC technique

| Parameter | N | | (D _m) | | (α) | | (Rs) | |
|--------------------------------|---------------------------|---------------------------|-------------------|---------------------------|---------------------------|------|--|-------------------------|
| | BUD _(Epimer B) | BUD _(Epimer A) | AZL | BUD _(Epimer B) | BUD _(Epimer A) | AZL | BUD _(B) /BUD _(A) | BUD _(B) /AZL |
| Ratio of organic modifier A/B* | 50:50 | 2389 | 449 | 428 | 459 | 0.59 | 7.80 | 1.07 |
| | 45:55 | 3598 | 1010 | 639 | 690 | 1.31 | 5.25 | 1.08 |
| | 42:58 | 3995 | 1038 | 875 | 956 | 1.68 | 5.69 | 1.09 |
| | 40:60 | 4202 | 1032 | 971 | 1064 | 2.09 | 5.08 | 1.10 |
| | 30:70 | 4101 | 936 | 1597 | 1749 | 3.00 | 5.83 | 1.09 |
| pH | 3.0 | 3946 | 995 | 940 | 1028 | 1.68 | 6.12 | 1.09 |
| | 3.5 | 4202 | 1032 | 971 | 1064 | 2.09 | 5.08 | 1.10 |
| | 4.0 | 4154 | 929 | 934 | 1027 | 2.36 | 4.35 | 1.10 |
| | 5.0 | 4141 | 731 | 899 | 983 | 3.45 | 2.85 | 1.09 |
| | 6.0 | 4119 | 775 | 935 | 1023 | 5.30 | 1.93 | 1.09 |
| Molar strength of buffer | 0.02 M | 3879 | 1681 | 1153 | 1219 | 4.47 | 2.73 | 1.06 |
| | 0.03 M | 3954 | 1161 | 1106 | 1199 | 3.40 | 3.52 | 1.08 |
| | 0.04 M | 4202 | 1032 | 971 | 1064 | 2.09 | 5.08 | 1.10 |
| | 0.05 M | 3774 | 436 | 893 | 988 | 0.97 | 10.2 | 1.11 |
| | | | | | | | | |

Where: A/B*, A is acetonitrile and B is phosphate buffer (0.04 M)

(N) is number of theoretical plates = $5.45 (t_R/W_{h/2})^2$

(D_m) is mass distribution ratio = $t_R - t_m/t_m$

(α) is selective factor = D_{m2}/D_{m1}

(Rs) is resolution = $2\Delta t_R/W_1 + W_2$

t_R is the retention time of the substance measured from the point of injection while t_m is the retention time of a non-retained marker

W_{h/2} is the peak width at the half height

W₁ and W₂ are the width of the peaks of the two components at their bases

Table 2 Analytical performance data for the simultaneous determination of BUD and AZL by the proposed HPLC and spectrophotometric methods

| Drug | BUD | | | | | AZL | |
|--|----------------------|--------------|--------------|---------------------|------------------------|-------------|----------------------|
| | HPLC method | | | First derivative | Ratio first derivative | HPLC method | Zero order method |
| | BUD sum epimer B + A | BUD epimer B | BUD epimer A | 265 nm | 270 nm | | 290 nm |
| Range of linearity ($\mu\text{g mL}^{-1}$) | 0.4–40.0 | | | 6.0–20.0 | 6.0–20.0 | 0.05–40.0 | 1.0–35.0 |
| Correlation coefficient (<i>r</i>) | 0.9999 | | | | | | |
| Slope (<i>a</i>) | 13.31 | 13.31 | 13.31 | 17×10^{-4} | 38×10^{-4} | 47.48 | 26×10^{-3} |
| Intercept (<i>b</i>) | −0.36 | −0.07 | −0.29 | 18×10^{-4} | -19×10^{-4} | 0.89 | 34×10^{-3} |
| % RSD ^a | 0.72 | 0.75 | 0.68 | 0.81 | 0.85 | 0.84 | 0.76 |
| % Error ^b | 0.25 | 0.27 | 0.24 | 0.29 | 0.3 | 0.30 | 0.24 |
| S.D. of residuals ($S_{y/x}$) | 0.844 | 0.429 | 0.415 | 19×10^{-5} | 45×10^{-5} | 0.23 | 26×10^{-4} |
| S.D. of intercept (S_a) | 0.457 | 0.233 | 0.225 | 22×10^{-5} | 4×10^{-5} | 0.111 | 136×10^{-5} |
| S.D. of slope (S_b) | 0.023 | 0.023 | 0.022 | 2×10^{-5} | 5×10^{-4} | 0.006 | 7×10^{-5} |
| LOD ($\mu\text{g mL}^{-1}$) ^c | 0.113 | 0.058 | 0.056 | 0.43 | 0.43 | 0.008 | 0.17 |
| LOQ ($\mu\text{g mL}^{-1}$) ^d | 0.343 | 0.175 | 0.170 | 1.29 | 1.32 | 0.023 | 0.52 |

^a Percentage relative standard deviation^b Percentage relative error^c Limit of detection^d Limit of quantitation

where PA is the peak area, C is the concentration of the drug ($\mu\text{g mL}^{-1}$), DA is the derivative amplitude, A is the absorbance and *r* is the correlation coefficient.

According to the analysis of the data [50], the regression equation's correlation coefficient (*r*) had a high value, and intercepts (*a*), slopes (*b*), standard deviations of intercept (S_a), standard deviations of slope (S_b), standard deviations of residuals ($S_{y/x}$), percentage relative standard deviation (% RSD), and percentage relative error (% Error) had a small values (Table 2). Low point scattering was observed in the data around the calibration curve.

Sensitivity of the method

According to ICH Q2 (R1) guidelines [49], the limit of quantitation (LOQ) and the limit of detection (LOD) were determined by employing the provided equations:

$$\text{LOQ} = 10 S_a/b \text{ and } \text{LOD} = 3.3 S_a/b.$$

where S_a =standard deviation of the intercept and *b*=slope of the calibration curve.

In the suggested methods, the values of LOQ and LOD for both BUD epimers B, A, and AZL were calculated and summarized in Table 2.

Accuracy

A comparison of the analytical data from the BUD and AZL laboratory assays with those obtained from HPLC comparison techniques was carried out in order to confirm the accuracy of the HPLC method [13, 40]. For statistical data analysis, student's *t*-test and variance ratio F-test were employed [50], ensuring that there is no significant difference in the findings as shown in Table 3. As well a standard addition method was applied to ensure the validity of the proposed spectrophotometric methods for the simultaneous determination of BUD and AZL in their laboratory-prepared dosage form. The recovery of both drugs (BUD and AZL) separately and in their combination was determined. In Tables 2 and 3; the comparison between the proposed methods and the reported one was performed by adopting Eq. 3 [the summation of the area under the curve (AUC) for both epimers].

For BUD, the recovery of BUD was calculated by adding a known concentration of the pure drug ($7.48 \mu\text{g mL}^{-1}$) to a previously analyzed nasal spray solution at three different concentrations (6.4, 7.0, and $8.18 \mu\text{g mL}^{-1}$). For each of the aforementioned nasal spray concentrations, the mentioned concentration of the pure BUD was added in separate flasks and the solution was then reanalyzed to determine the total amount of the drug. The approach

Table 3 Comparative analytical resulted data for determination of BUD and AZL in pure form by the proposed HPLC and comparison methods

| Parameter | BUD | | AZL | |
|-------------------------|-------------------|------------------------|------------------|------------------------|
| | Proposed method | Comparison method [13] | Proposed method | Comparison method [40] |
| $\bar{X} \pm \text{SD}$ | 100.29 \pm 0.75 | 99.95 \pm 1.36 | 99.85 \pm 0.84 | 99.61 \pm 0.98 |
| t-value | 0.58 (1.81) | | 0.45 (1.81) | |
| F-value | 3.28 (4.35) | | 1.37 (4.35) | |

Each result is the mean recovery of three separate determinations

Figures between brackets are the tabulated t and F-values at (P = 0.05)

was performed in triplicate adopting the procedure as described below “Construction of calibration curves”.

For AZL, the recovery was determined by adding a known amount of pure drug ($32.0 \mu\text{g mL}^{-1}$) to a previously analyzed nasal spray solution at three different concentrations (27.4, 30.0, $35.0 \mu\text{g mL}^{-1}$) in separate flasks, and the solution was reanalyzed for the total drug concentration. The approach was performed in triplicate adopting the procedure as outlined below “Construction of calibration curves”.

For estimation of BUD and AZL in their combination, the addition of both pure drugs in a ratio of 1:4.28 ($7.48 \mu\text{g mL}^{-1}$ and $32.0 \mu\text{g mL}^{-1}$) for BUD and AZL, respectively was performed, then previously analyzed nasal spray solutions of both drugs were added at three different concentrations (6.4, 7.0, 8.18), (27.4, 30.0, 35.0) for BUD and AZL, respectively. For each of the aforementioned nasal spray concentrations, the mentioned concentration of both pure drugs was added in separate flasks and the solution was then reanalyzed to determine the total concentration of the drugs. The approach was performed in triplicate utilizing the procedure as mentioned below “Construction of calibration curves”. The obtained results were shown in Additional file 1: Table S1.

Precision

The intra-day and inter-day precision for the proposed methods were performed by assaying three different concentrations for both drugs in 1 day and for 5 consecutive days. Where, in the HPLC method analysis of BUD and AZL was performed using three distinct concentrations of (12, 15, and $18 \mu\text{g mL}^{-1}$) for both BUD and AZL. While in the spectrophotometric methods triplicate assay of BUD and AZL at (10, 13, and $16 \mu\text{g mL}^{-1}$) and at (12, 15, and $18 \mu\text{g mL}^{-1}$), respectively. The low values of SD and % RSD as shown in Additional file 1: Table S2 demonstrate the good precision of the suggested approaches.

Robustness

The suggested chromatographic method's robustness was assessed to guarantee its reliability in the analytical application. Slight variations in one of the variables were

performed while the others were kept constant, including the pH of the mobile phase (3.5 ± 0.2) and the percentage of organic modifiers ($40.0\% \pm 1\%$). The efficiency of separation and resolution of BUD epimers and AZL was undisturbed by the results gathered from these slight alterations, indicating the reliability of the suggested technique.

Applications

Analysis of BUD/AZL in their synthetic mixtures and dosage forms The suggested approaches were furthermore operated for simultaneous estimation of BUD and AZL in the ratio of (1:4.28) for (BUD: AZL) in their laboratory synthetic mixture and their dosage form. The analyses were carried out in triplicate at three different concentrations 1.7, 3.2, and $6.4 \mu\text{g mL}^{-1}$ for BUD and 6.85, 13.7 and $27.4 \mu\text{g mL}^{-1}$ for AZL in the HPLC method. As well as 6.4, 7.0, and $8.18 \mu\text{g mL}^{-1}$ for BUD and 27.4, 30.0, and $35.0 \mu\text{g mL}^{-1}$ for AZL in spectrophotometric methods; the same procedures were performed as described below “Construction of calibration graphs”. The application of the proposed method for the determination of BUD concentration in the laboratory-prepared mixture and dosage form was afforded by summation of the AUC of the two epimers peaks consequently Eq. (3) was utilized. The obtained statistical data were adequate, as indicated by the low values of SD as summarized in Table 4. The representative chromatograms constructed from the application of both laboratory synthetic mixture and laboratory-prepared dosage form were shown in Additional file 1: Figs. S1 and S2.

Greenness assessment applying AGREE approach

Various approaches are utilized for evaluating the greenness of analytical assays, however, only AGREE software utilizes all 12 GAC principles for greenness determination [51]. Therefore, the greenness of the approaches was assessed by AGREE: The Analytical Greenness Calculator (version 0.5, Gdansk University of Technology, Gdansk, Poland, 2020). Figure 6 illustrates a representative

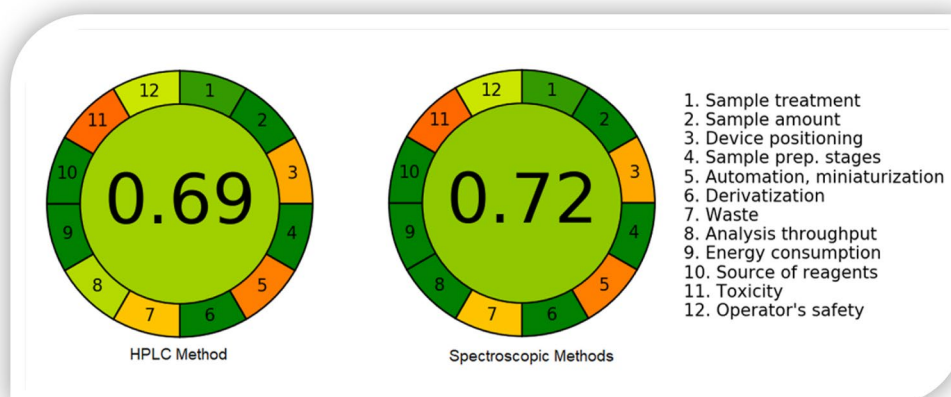
Table 4 Comparative analytical resulted data from simultaneous determination of BUD and AZL in their laboratory synthetic mixture and laboratory prepared dosage form by the proposed HPLC and spectrophotometry methods

| HPLC method | | | | | | | | |
|-------------|------------------|------------------------------|------------------|----------------------------|---------------------------------|-----|----------------------------|-------------------|
| Parameter | | Laboratory synthetic mixture | | | Laboratory prepared dosage form | | | |
| | | Proposed method | | Comparison method [13, 40] | Proposed method | | Comparison method [13, 40] | |
| BUD + AZL | $\bar{X} \pm SD$ | BUD | 99.52 \pm 0.21 | 99.3 \pm 0.58 | Rhino aqua and Zalastin | BUD | 99.39 \pm 0.24 | 100.30 \pm 0.87 |
| | | AZL | 99.85 \pm 0.23 | 99.59 \pm 0.61 | | AZL | 100.10 \pm 0.67 | 99.97 \pm 0.42 |
| t-value | | BUD | 0.62 (2.13) | | | BUD | 1.75 (2.13) | |
| | | AZL | 0.7 (2.13) | | | AZL | 0.29 (2.13) | |
| F-value | | BUD | 7.16 (19.0) | | | BUD | 12.61 (19.0) | |
| | | AZL | 6.9 (19.0) | | | AZL | 2.62 (19.0) | |

| Spectrophotometric methods | | | | | | | | |
|----------------------------|------------------|------------------------------|-------------------|------------------|---------------------------------|------------------|-------------------|------------------|
| | | Laboratory synthetic mixture | | | Laboratory prepared dosage form | | | |
| | | BUD | | AZL | BUD | | AZL | |
| | | $^1D_{265}$ | $^1DD_{270}$ | $^0D_{290}$ | $^1D_{265}$ | $^1DD_{270}$ | $^0D_{290}$ | |
| BUD + AZL | $\bar{X} \pm SD$ | 99.87 \pm 0.37 | 100.03 \pm 0.26 | 99.88 \pm 0.25 | Rhino aqua and Zalastin | 99.86 \pm 0.46 | 100.12 \pm 0.52 | 99.93 \pm 0.19 |

Each result is the mean recovery of three separate determinations

Figures between brackets are the tabulated *t* and *F*-values at (*P* = 0.05)

**Fig. 6** Representative pictograms for AGREE scores for HPLC and spectroscopic methods that obtained using the Analytical Greenness Calculator (AGREE) approach

pictogram for the AGREE score of the proposed chromatographic and spectroscopic methods. For the chromatographic, the AGREE score was calculated to be 0.66, while for the spectroscopic methods utilized for the determination, the AGREE score was found to be 0.72. Both values revealed a good greenness of the proposed approaches.

Greenness assessment applying the green analytical procedure index (GAPI) approach

GAPI is another approach applied to evaluate the greenness of the analytical methodology [52]. Five pentagrams were constructed and colored according to the degree of the environmental effect regarding the different factors. The green color indicates low environmental impact, the yellow color reflects medium environmental impact,

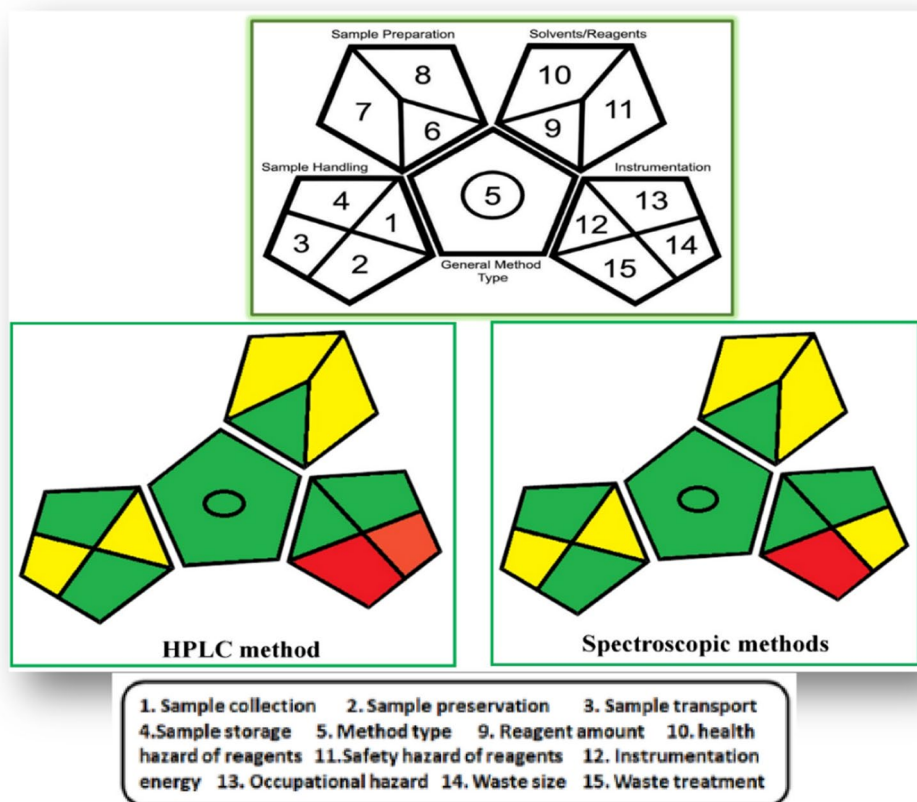


Fig. 7 Representative pictograms for HPLC and spectroscopic methods that obtained using green analytical procedure index (GAPI) approach

and the red color expresses high environmental effect. The excellence of this approach, as well as its capacity to clearly identify the weakest aspects of the conducted operation, motivated us to use it to assess the greenness of the suggested methodologies as shown in (Fig. 7). Both studies revealed that we have to reduce the amount of acetonitrile as a hazardous solvent to enhance the greenness of the proposed methods and decrease waste and toxicity in future studies.

Conclusion

Efficient, economic, and green chromatographic and spectrophotometric methods were established for the estimation of a novel combination of BUD/AZL that is used successfully for the curing of allergic rhinitis and relieving its symptoms. BUD is an important inhalation corticosteroid for chronic asthmatic patients, and it was found to have an essential role in the inhibition of COVID-19 replication and cytokine production. The proposed spectroscopic and chromatographic methods are applied effectively to estimate and separate this mixture. The separation of BUD epimers and AZL was afforded by the proposed chromatographic approach with excellent performance in a relatively short elution

time and satisfactory resolution. Besides, three spectrophotometric methods were utilized for the estimation of this mixture by zero order, first order derivative, and ratio first derivative methods. The suggested methods were validated and further applied for the quantification of BUD/AZL in their laboratory-prepared mixture and dosage form according to the recommended ratio of 1:4:28. The AGREE and GAPI metrics were approved an excellent greenness of the proposed approaches.

Abbreviations

| | |
|-----------|--|
| A | Absorbance |
| ACE2 | Angiotensin-converting enzyme 2 |
| AUC | The area under the curve |
| AZL | Azelastine |
| BUD | Budesonide |
| COPD | Chronic obstructive pulmonary disease |
| C | Concentration |
| r | Correlation coefficient. |
| COVID-19 | Coronavirus disease 2019 |
| DA | Derivative amplitude |
| EKCC | Electrokinetic capillary chromatography |
| GC | Gas chromatography |
| GAPI | Greenness assessment applying the green analytical procedure index |
| HPLC | High-performance liquid chromatography |
| HPTLC | High-performance thin-layer chromatography |
| HCoV-229E | Human coronavirus 229E |

| | |
|-----------------------|--|
| ICS | Inhaled corticosteroids |
| IFN | Interferon |
| a | Intercepts of the calibration curve. |
| LC/MS/MS | Liquid chromatography with tandem mass spectrometry |
| LOQ | Limit of quantitation |
| LOD | Limit of detection |
| $\mu\text{g mL}^{-1}$ | Microgram per millimeter |
| PA | Peak area |
| % RSD | Percentage relative standard deviation |
| % Error | Percentage relative error |
| b | Slopes of the calibration curve |
| S_a | Standard deviation of the intercept |
| S_b | Standard deviation of the slope |
| S_y/x | Standard deviations of residuals |
| AGREE | The Analytical Greenness Calculator |
| EKB | The Egyptian Knowledge Bank |
| STDF | The Science, Technology & Innovation Funding Authority |
| TNSS | Total nasal symptom score |
| UPLC/MS/MS | Ultra-high-performance liquid chromatography with tandem mass spectrometry |

Supplementary Information

The online version contains supplementary material available at <https://doi.org/10.1186/s13065-023-00936-z>.

Additional file 1: Figure S1. Typical Chromatogram for the separation of BUD ($6.4 \mu\text{g mL}^{-1}$) [BUD Epimer B; 8.03 min, BUD Epimer A; 8.73 min] and AZL ($27.4 \mu\text{g mL}^{-1}$, 2.32 min) in their laboratory synthetic mixture. Where; (1) Solvent Front, (2) AZL (3) BUD Epimer B (4) BUD Epimer A.

Figure S2. Typical Chromatogram for the separation of BUD ($6.4 \mu\text{g mL}^{-1}$) [BUD Epimer B; 8.03 min, BUD Epimer A; 8.8 min] and AZL ($27.4 \mu\text{g mL}^{-1}$, 2.32 min) in laboratory prepared dosage form (Rhino Aqua and Zalastin). Where; (1) Solvent Front, (3) AZL (5) BUD Epimer B (6) BUD Epimer A.

Table S1. Standard Addition Test Results for Spectrophotometric First Derivative, Ratio First Derivative and Zero Order for Determination of BUD and AZL in their Nasal Spray Solutions. **Table S2.** Intra-day and inter-day precision data for the determination of BUD and AZL in pure form by the HPLC and methods.

Acknowledgements

Not applicable.

Author contributions

MEAH: conceptualization, visualization, supervision, investigation, and writing—original draft. AAE-M: conceptualization, methodology, data analysis, and validation. SME-A: conceptualization, and supervision. DRE-W: conceptualization, methodology and supervision. All the authors have reviewed the manuscript. All authors read and approved the final manuscript.

Funding

Open access funding provided by The Science, Technology & Innovation Funding Authority (STDF) in cooperation with The Egyptian Knowledge Bank (EKB). This work wasn't funded by any third party.

Availability of data and materials

Datasets generated and/or analyzed during the current study are available from the corresponding author upon reasonable request.

Declarations

Ethics approval and consent to participate

Not applicable.

Consent for publication

Not applicable.

Competing interests

The authors declare that they have no known competing financial interests or personal relationships that could have appeared to influence the work reported in this paper.

Author details

¹Department of Medicinal Chemistry, Faculty of Pharmacy, Mansoura University, Mansoura 35516, Egypt. ²Department of Pharmaceutical Chemistry, Faculty of Pharmacy, Horus University - Egypt, New Damietta, Egypt. ³Department of Pharmaceutical Chemistry, Faculty of Pharmacy, Delta University for Science and Technology, Gamasa 35712, Egypt.

Received: 19 October 2022 Accepted: 3 March 2023

Published online: 14 March 2023

References

- British Pharmacopoeia Commission. British Pharmacopoeia. London: Her Majesty's Stationary Office; 2012. p. 199–200.
- Beale JM, Block J, Hill R. Organic medicinal and pharmaceutical chemistry. Philadelphia: Lippincott Williams & Wilkins; 2010.
- Szefer SJ. Pharmacodynamics and pharmacokinetics of budesonide: a new nebulized corticosteroid. J Allergy Clin Immunol. 1999;104(4):S175–83.
- Yamaya M, Nishimura H, Deng X, Sugawara M, Watanabe O, Nomura K, Shimotai Y, Momma H, Ichinose M, Kawase T. Inhibitory effects of glycopyrronium, formoterol, and budesonide on coronavirus HCoV-229E replication and cytokine production by primary cultures of human nasal and tracheal epithelial cells. J Respir Investig. 2020;58(3):155–68.
- Finney LJ, Glanville N, Farne H, Aniscenko J, Fenwick P, Kemp SV, Trujillo-Torralbo M-B, Loo SL, Calderazzo MA, Wedzicha JA. Inhaled corticosteroids downregulate the SARS-CoV-2 receptor ACE2 in COPD through suppression of type I interferon. J Allergy Clin Immunol. 2020;147(2):510–519.e515.
- Peters MC, Sajuthi S, Deford P, Christenson S, Rios CL, Montgomery MT, Woodruff PG, Mauger DT, Erzurum SC, Johansson MW. Eratume: COVID-19-related genes in sputum cells in asthma. Relationship to demographic features and corticosteroids. Am J Respir Crit Care Med. 2020;202(1):83–90.
- Higham A, Mathioudakis A, Vestbo J, Singh D. COVID-19 and COPD: a narrative review of the basic science and clinical outcomes. Eur Respir Rev. 2020. <https://doi.org/10.1183/16000617.0199-2020>.
- Sanap D, Sisodia A, Patil S, Janjale M. Novel and validated spectrophotometric determination of budesonide from bulk and tablets using mixed hydrotropic solubilization technique. Int J Pharm Sci Res. 2011;2(9):2419.
- Bharti P, Sachan N, Chandra P, Gahlo K, Gouda MM, Shabaraya AR, Shantakumar S, Shyale SS, Kumar PR. Development and validation of selective UV spectrophotometric analytical method for budesonide pure sample. J Appl Pharm Sci. 2011;01(07):158–61.
- Joshi M, Misra A. Spectrophotometric determination of budesonide. Indian J Pharm Sci. 2000;62(2):92.
- Gurjar NM, Seth A, Zanwar A, Patel J, Deshmukh G. Development of first derivative spectroscopy method for estimation of budesonide and formoterol in combined dosage form. Pharma Sci Monitor. 2012;3(1):82–92.
- Prasad A. Simultaneous spectrophotometric determination of formoterol fumarate and budesonide in their combined dosage form. Indian J Chem Technol. 2006;13:81–3.
- Salem Y, Shaldam M, El-Sherbiny D, El-Wasseef D, El-Ashry S. Simultaneous determination of formoterol fumarate and budesonide epimers in metered dose inhaler using ion-pair chromatography. J Chromatogr Sci. 2017;55(10):1013–20.
- Kale NR, Pingle AP, Mirza JA, Dhongade GN. Development and validation of stability-indicating RP-HPLC method for simultaneous estimation of formoterol fumarate and budesonide in metered dose inhaler formulation. World J Pharm Res. 2014;3:1386–400.
- Pai N, Suhas S. Development and validation of RP-HPLC method for estimation of formoterol fumarate and budesonide in pressurised meter dose inhaler form. Der Pharm Sin. 2013;4:15–26.

16. Dave HN, Makwana AG, Suhagia BN. Validated reversed phase high performance liquid chromatographic method for determination of three novel steroids in bulk and pressurized metered-dose commercial preparations using a common mobile phase. *Int J Appl Sci Eng*. 2013;11(2):125–35.
17. Srinivasaro K, Gorule V, Akula VK. Development and validation for simultaneous estimation of budesonide and salmeterol xinafoate in metered dose inhalation form by RP-HPLC. *Int J Pharm Phytopharmacol Res*. 2012;1(5):271–5.
18. Blewett AJ, Varma D, Gilles T, Butcher R, Jacob J, Amazan J, Jansen SA. Development and validation of a stability-indicating high-performance liquid chromatography method for the simultaneous determination of albuterol, budesonide, and ipratropium bromide in compounded nebulizer solutions. *J AOAC Int*. 2011;94(1):110–7.
19. Sahib MN, Darwis Y, Khiang PK, Tan YTF. Aerodynamic characterization of marketed inhaler dosage forms: high performance liquid chromatography assay method for the determination of budesonide. *Afr J Pharm Pharmacol*. 2010;4(12):878–84.
20. Gupta M, Bhargava HN. Development and validation of a high-performance liquid chromatographic method for the analysis of budesonide. *J Pharm Biomed Anal*. 2006;40(2):423–8.
21. Buscher B, Jägfeldt H, Sandman H, Brust-van Schaik R, Van Schaik F, Brüll L. The determination of budesonide and fluticasone in human sputum samples collected from COPD patients using LC–MS/MS. *J Chromatogr B*. 2012;880:6–11.
22. Szeitz A, Manji J, Riggs KW, Thamboo A, Javer AR. Validated assay for the simultaneous determination of cortisol and budesonide in human plasma using ultra high performance liquid chromatography–tandem mass spectrometry. *J Pharm Biomed Anal*. 2014;90(Supplement C):198–206.
23. Lu Y, Sun Z, Zhang Y, Chen X, Zhong D. Simultaneous quantification of 22R and 22S epimers of budesonide in human plasma by ultra-high-performance liquid chromatography–tandem mass spectrometry: application in a stereoselective pharmacokinetic study. *J Chromatogr B Anal Technol Biomed Life Sci*. 2013;921–922:27–34.
24. Krzek J, Czekaj JS, Rzeszutko W, Jonczyk A. Direct separation, identification and quantification of epimers 22R and 22S of budesonide by capillary gas chromatography on a short analytical column with Rtx-5 stationary phase. *J Chromatogr B Anal Technol Biomed Life Sci*. 2004;803(2):191–200.
25. El-Masry AA, Hammouda MEA, El-Wasseef DR, El-Ashry SM. Validated spectroscopic methods for determination of anti-histaminic drug azelastine in pure form: analytical application for quality control of its pharmaceutical preparations. *Spectrochim Acta Part A Mol Biomol Spectrosc*. 2018;191:413–20.
26. Gouda AA, El Sheikh R, El Saied H. Extractive spectrophotometric determination of azelastine hydrochloride in pure form and pharmaceutical formulations. *Can Chem Trans*. 2015;3:29–41.
27. Salama NN, Abdel-Razeq SA, Abdel-Atty S, El-Kosy N. Spectrophotometric determination and thermodynamic studies of the charge transfer complexes of azelastine-HCl. *Bull Fac Pharm Cairo Univ*. 2011;49(1):13–8.
28. Elghobashy M, Badran U, Salem M, Kelani K. Stability indicating spectrophotometric and chromatographic methods for the determination of azelastine hydrochloride in presence of its alkaline degradant. *Anal Chem Indian J*. 2014;14(4):135–42.
29. Hassouna MEAM, Mohamed MA. Determination of azelastine hydrochloride and benzalkonium chloride in their ophthalmic solution by different spectrophotometric methods. *World J Appl Chem*. 2017;2(2):48–56.
30. Merey HA, El-Mosallany SS, Hassan NY, El-Zeany BA. Simultaneous determination of fluticasone propionate and azelastine hydrochloride in the presence of pharmaceutical dosage form additives. *Spectrochim Acta Part A Mol Biomol Spectrosc*. 2016;160:50–7.
31. Patel SG, Patel KV, Shah PA, Patel KG. Ratio derivative spectrophotometric method for the simultaneous determination of two binary mixtures in pharmaceutical dosage form. *Indian J Drugs*. 2019;7(4):122–32.
32. El-Masry AA, Hammouda MEA, El-Wasseef DR, El-Ashry SM. Validated sensitive spectrofluorimetric method for determination of antihistaminic drug azelastine HCl in pure form and in pharmaceutical dosage forms: application to stability study. *Luminescence*. 2017;32(2):177–81.
33. Elghobashy MR, Badran OM, Salem MY, Kelani KM. Application of membrane selective electrodes for the determination of azelastine hydrochloride in the presence of its alkaline degradant in eye drops and plasma. *Anal Bioanal Electrochem*. 2013;5(3):325–40.
34. Abdel-Razeq SA, Foad MM, Salama NN, Abdel-Atty S, El-Kosy N. Voltammetric determination of azelastine-HCl and emedastine difumarate in micellar solution at glassy carbon and carbon paste electrodes. *Sens Electroanal*. 2011;6:289–305.
35. Singh G, Rani S. Determination of azelastine in different samples by poly (vinyl chloride) based membrane electrode. *Asian J Pharm Anal*. 2013;3(2):37–41.
36. Salama NN, Abdel-Razeq SA, Abdel-Atty S, El-Kosy N. Development and validation of densitometry TLC stability indicating method for quantitative determination of azelastine hydrochloride and emedastine difumarate in their drug products. *Br J Pharm Res*. 2014;4(1):79.
37. Wyszomirska E, Czerwińska K, Kublin EL, Mazurek AP. Identification and determination of ketotifen hydrogen fumarate, azelastine hydrochloride, dimetindene maleate and promethazine hydrochloride by densitometric method. *Acta Pol Pharm Drug Res*. 2013;70(6):951.
38. El-Shaheny RN, Yamada K. Stability study of the antihistamine drug azelastine HCl along with a kinetic investigation and the identification of new degradation products. *Anal Sci*. 2014;30(6):691–7.
39. da Costa LM, Oliveira de Almeida Leite H, Kassab NM, Singh AK. Green analytical methods for the separation of seven antihistamines: application in separation of azelastine and related impurities in nasal solution. *Int J Anal Chem*. 2019. <https://doi.org/10.1155/2019/9489723>.
40. Rao KLN, Reddy KP, Babu KS, Raju KS, Rao KV, Shaik JV. Simultaneous estimation of fluticasone propionate, azelastine hydrochloride, phenylethyl alcohol and benzalkonium chloride by RP-HPLC method in nasal spray preparations. *J Res Pharm Sci*. 2010;1(4):473–80.
41. Thangabalan B, Kumar PV. RP-HPLC determination of azelastine in pure form and in ophthalmic formulation. *Int J Pharm Sci Rev Res*. 2012;17:62–4.
42. Dubey R, Das S, Roychowdhury S, Pradhan KK, Ghosh M. Validated HPTLC method for the determination of azelastine hydrochloride in bulk drug and dosage form. *Pharmbit*. 2013;27:9–11.
43. Park Y-S, Kim S-H, Kim Y-J, Yang S-C, Lee M-H, Shaw LM, Kang J-S. Determination of azelastine in human plasma by validated liquid chromatography coupled to tandem mass spectrometry (LC-ESI/MS/MS) for the clinical studies. *Int J Biomed Sci*. 2010;6(2):120.
44. Heinemann U, Blaschke G, Knebel N. Simultaneous enantioselective separation of azelastine and three of its metabolites for the investigation of the enantiomeric metabolism in rats: 1. Liquid chromatography–ionspray tandem mass spectrometry and electrokinetic capillary chromatography. *J Chromatogr B*. 2003;793(2):389–404.
45. Azelastine/budesonide intranasal - Sedor. *AdisInsight drugs*. Released 05 Feb 2009; updated 04 Oct 2017. <https://adisinsight.springer.com/drugs/800029620>.
46. Patel P, Salapatek A, D'Angelo P, Bates M, Patel D, Zimmerman R, Pipkin JD. The combination product Captisol-Enabled® budesonide + azelastine HCl nasal spray provides significant, long-lasting relief of ocular allergy symptoms in ragweed allergic patients studied in an environmental exposure chamber (EEC). *J Allergy Clin Immunol*. 2009;123(2):S130.
47. Moffat AC, Osselton MD, Widdop B, Watts J. Clarke's analysis of drugs and poisons, vol. 3. London: Pharmaceutical Press; 2011.
48. Slack RJ, Hart AD, Luttmann MA, Clark KL, Begg M. In vitro characterisation of the duration of action of the histamine-1 receptor antagonist azelastine. *J Eur J Pharmacol*. 2011;670(2–3):586–92.
49. Branch SK. Guidelines from the international conference on harmonisation (ICH). *J Pharm Biomed Anal*. 2005;38(5):798–805.
50. Miller J, Miller JC. Statistics and chemometrics for analytical chemistry. Harlow: Pearson Education; 2018.
51. Pena-Pereira F, Wojnowski W, Tobiszewski M. AGREE—analytical GREENness metric approach and software. *Anal Chem*. 2020;92(14):10076–82.
52. Plotka-Wasyłka J. A new tool for the evaluation of the analytical procedure: green analytical procedure index. *Talanta*. 2018;181:204–9.

Publisher's Note

Springer Nature remains neutral with regard to jurisdictional claims in published maps and institutional affiliations.